Available online at www.sciencedirect.com
ScienceDirect
Ceramics International 35 (2009) 3503–3506
CERAMICS INTERNATIONAL
www.elsevier.com/locate/ceramint

Short communication

Non-isothermal crystallization kinetics of $MgO–BaO–B_2O_3–Al_2O_3–SiO_2$ glass

Yin Cheng [a,*], Hanning Xiao [a,b], Bingzhong Tang [a]

[a] College of Physics and Electronic Science, Changsha University of Science & Technology, Changsha 410004, China
[b] College of Materials Science and Engineering, Hunan University, Changsha 410082, China

Received 17 November 2008; received in revised form 12 March 2009; accepted 2 May 2009
Available online 6 June 2009

Abstract

$5MgO–9BaO–33B_2O_3–33Al_2O_3–20SiO_2$ (mol%) glass was prepared by the melt quenching method at 1823 K for 2 h. Dilatometry and differential scanning calorimetry (DSC) curves of the glass have been investigated. Fragility index F was used to estimate glass formability. The crystallization kinetics of the glass was described by the activation energy (E) for crystallization and numerical factors (n, m) depending on the nucleation process and growth morphology. XRD and SEM analysis were also used to describe the crystals' types and morphology precipitated from the $MgO–BaO–B_2O_3–Al_2O_3–SiO_2$ glass. The results show that the effective activation energy of the crystallization process E was 45.19 kJ/mol, and n up to 4.05. Two crystals phases, i.e. $Al_4B_2O_9$ and $Al_{20}B_4O_{36}$ were observed in the crystallized samples. SEM results were consistent with crystallization kinetics.

Keywords: Non-isothermal; Crystallization; DSC

1. Introduction

Glasses and glass–ceramics in the $B_2O_3–Al_2O_3–SiO_2$ system have been widely investigated for various technological applications like low-cost optical connectors, dielectrics and sealant materials for solid oxide fuel cells [1–3]. In order to obtain a fine microstructure, intensive nucleation and crystallization are essential. Although a number of studies have been reported aimed specifically at examining the relationship between nucleation and crystallization in the derivatives of the $B_2O_3–Al_2O_3–SiO_2$ glass system [4–6], a literature survey reveals that there is still need of comprehensive data on the crystallization kinetics of the glasses in the $MgO–BaO–Al_2O_3–B_2O_3–SiO_2$ system. In view of the above-mentioned perspective, the present work has been undertaken to study the thermal properties, the crystallization kinetics and the crystallization sequences of the glass $5MgO–9BaO–33B_2O_3–33Al_2O_3–20SiO_2$ (mol%).

2. Experimental

Reagent grade $MgCO_3$, $BaCO_3$, Al_2O_3, H_3BO_3 and SiO_2 powders were used. Homogeneous mixtures of batches (~100 g), obtained by ball milling, were preheated at 1173 K for 1 h for decarbonization and then melted in platinum crucible at 1823 K for 2 h in air. The resulting melt was quenched in graphite mould and immediately annealed at 823 K (i.e., close to the transformation temperature T_g) for 1 h. A portion of the frit was handmilled in an agate pestle mortar to obtain the glass powder for the thermal analysis. Crystallization kinetics of the glass powder was studied by differential scanning calorimetry (DSC) in a Netzsch STA449C calorimeter at different heating rates (10, 20, 30, 40 K/min). The crystallized phases of reheated samples were analyzed by X-ray Diffraction (XRD) using Cu Kα radiation in a Rigaku D/Max 2550VB+ equipment with a rotating anode. After immerging in 1 wt.% HF solution for 3–5 min, microstructures of reheated samples were observed by SEM methods using JEOL JSM-6700F electron microscope, operating in the secondary electron emission mode.

* Corresponding author. Tel.: +86 731 5258232; fax: +86 731 2617678.
E-mail address: zjbcy@126.com (Y. Cheng).

0272-8842/$36.00.
doi:10.1016/j.ceramint.2009.05.010

3. Results and discussion

3.1. Glass transition

Eq. (1) has been used for the glass transition according to Kissinger's formula [7], which has often been used to calculate the activation energy of transition E_g.

$$\ln\left(\frac{T_g^2}{\beta}\right) = \frac{E_g}{RT_g} + \text{const.} \quad (1)$$

where T_g is glass transition temperature, β is the heating rate and R is the universal gas constant. Fig. 1 shows the plots of $\ln T_g^2/\beta$ versus $1/T_g$ for the glass powder displaying the linearity of the equations used. According to Eq. (1), the value of the activation energy obtained for the glass transition is 206.1 kJ/mol.

The fragility index can be calculated using the following relation [8]:

$$F = \frac{E_g}{T_g \ln 10} \quad (2)$$

where E_g is the activation energy for glass transition. Calculated by Eq. (2), the value of fragility index (F) for glass at heating rate of 10 K/min is 9.6. This indicates that the glass is obtained from a kinetically strong-glass forming (KS) liquid [9].

3.2. Crystallization kinetics

Fig. 2 is a typical scan at heating rate of 20 K/min showing T_g and crystallization peak temperature T_p. Values of characteristic temperatures summarized in Table 1 were extracted using the Proteus software installed in the DSC instrument. Both the transition and crystallization temperatures are seen to increase as heating rate increased.

The average values of E_G (the activation energies for crystal growth) were evaluated by the Šatava method [10]:

$$\left.\frac{\mathrm{d}\ln[-\ln(1-x)]}{\mathrm{d}(1/T)}\right|_{\beta} = -1.052\frac{mE_G}{R} \quad (3)$$

where n and m are factors depending on the nucleation process and growth morphology [10]. The volume fraction x of each sample is given by the area of the crystallization exothermic peak [11], which lies in the range of 0.1–0.9 as shown in Fig. 3. The effective activation energy of the crystallization process E can be defined by $E = (m/n)E_G$, which were calculated by the

Table 1
Thermal characteristics of MgO–BaO–B_2O_3–Al_2O_3–SiO_2 glass.

β (K/min)	T_g (K)	T_p (K)
10	932.5	1068.5
20	951.3	1087.2
30	967.2	1095.6
40	979.5	1104.3

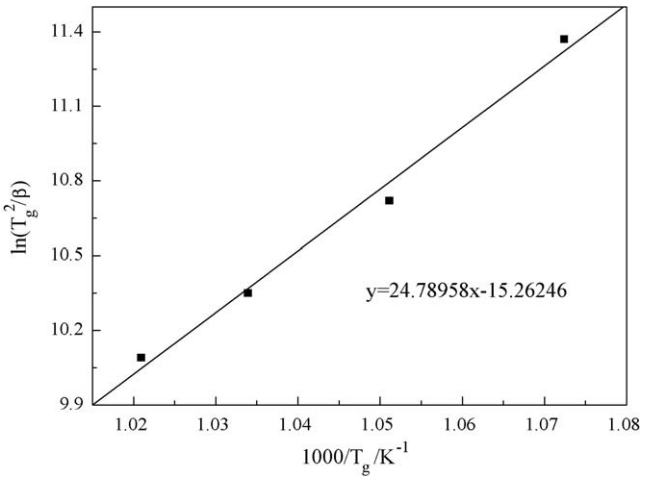

Fig. 1. Plots of $\ln T_g^2/\beta$ versus $1/T_g$ for determination of E_g at different heating rates β.

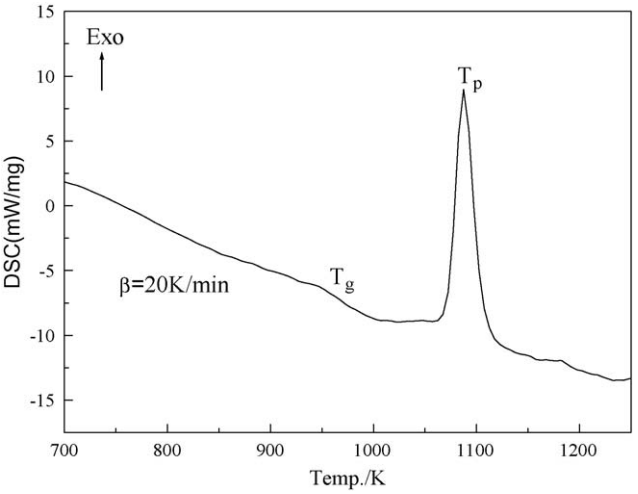

Fig. 2. DSC curve at heating rate of 20 K/min.

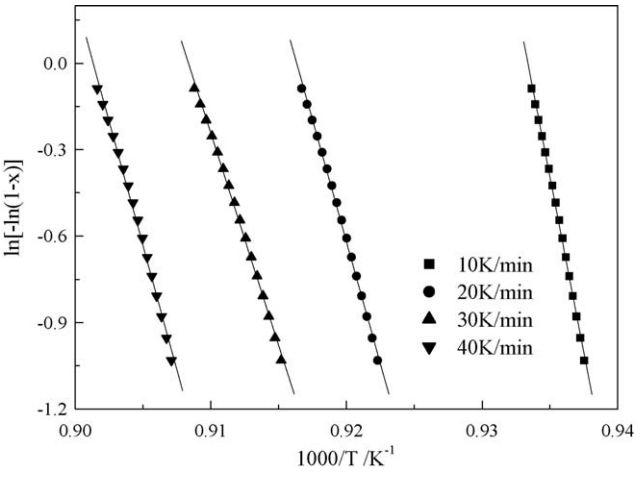

Fig. 3. Determination of mE_G according to the Šatava method by plotting $\ln[-\ln(1-x)]$ *vs.* $1/T$ at different heating rates.

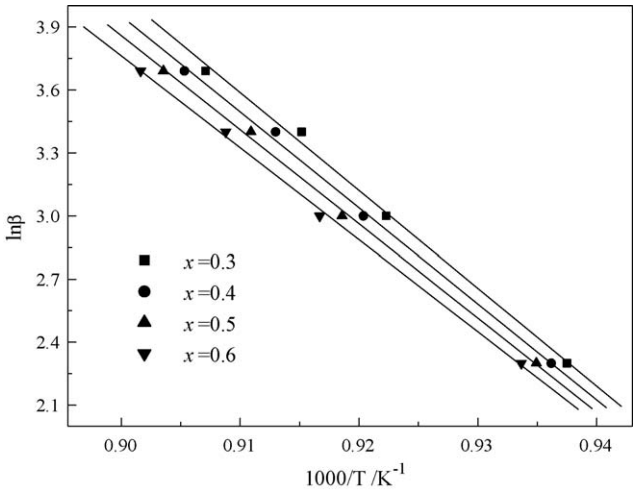

Fig. 4. Ozawa–Chen plots (ln β *vs.* $1/T_x$) for determination of $E = (m/n)E_G$ at different values of x.

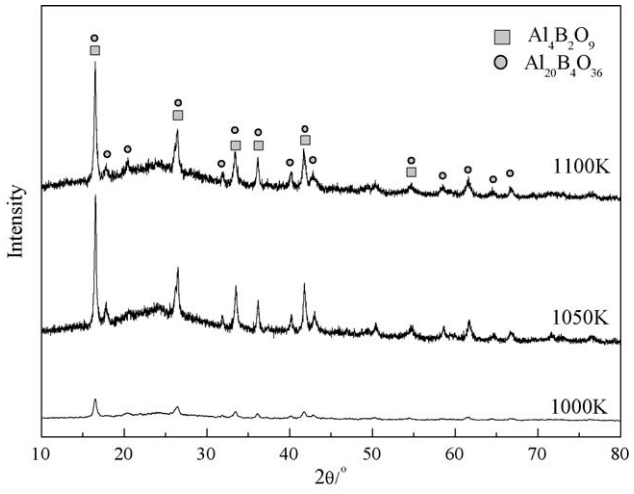

Fig. 5. XRD patterns of crystallized samples heat-treated at 1000–1100 K for 1 h.

Ozawa–Chen method [12,13]:

$$\left.\frac{d(\ln\beta)}{d(1/T)}\right|_{\chi} = -1.052\frac{m}{n}\frac{E_G}{R} \quad (4)$$

at the constant x of 0.3, 0.4, 0.5 and 0.6, respectively, as shown in Fig. 4. The mean values at different values of x were accepted as E in the glasses listed in Table 2.

The values of n, m and E_G were estimated by combining the results above, assuming that nucleation rate to be constant ($n = m + 1$). All values of the kinetic parameters of crystallization above were summarized in Table 2. It can be seen that E is 45.19 kJ/mol, showing good crystallization ability of the investigated glass. The values of n and m depend on the mechanism of the crystallization reaction as shown in Table 3. In the investigated system, n equals to 4.05. Thus the crystallization of MgO–BaO– B_2O_3–Al_2O_3–SiO_2 glass is controlled by a three-dimensional growth mechanism.

3.3. Crystals phases

Fig. 5 shows the XRD pattern of crystallized glass heat-treated at 1000, 1050 and 1100 K for 1 h, respectively. Only one main crystal phase, $Al_4B_2O_9$, was observed in 1000 K crystallized sample, while two crystal phases, $Al_4B_2O_9$ and $Al_{20}B_4O_{36}$ were observed in the other crystallized samples. The two latter samples have much higher crystal content than the former according to the height of diffraction peaks. This indicates that $Al_4B_2O_9$ was precipitated first from the glass matrix at about 1000 K. According to the results of previous studies [14,15], the following reaction possibly took place in the heating process:

$$5Al_4B_2O_9 \rightarrow Al_{20}B_4O_{36} + 3B_2O_3\uparrow$$

Table 2
Kinetic parameters of crystallization calculated by different methods.

n	m	mE_G (kJ/mol)	E_G (kJ/mol)	$E = (m/n)E_G$ (kJ/mol)
4.05	1	183.09	60.3	45.19

Table 3
The values of n and m for various crystallization mechanisms.

Mechanism	n	m
Bulk crystallization		
Three-dimensional growth	4	3
Two-dimensional growth	3	2
One-dimensional growth	2	1
Surface crystallization	1	1

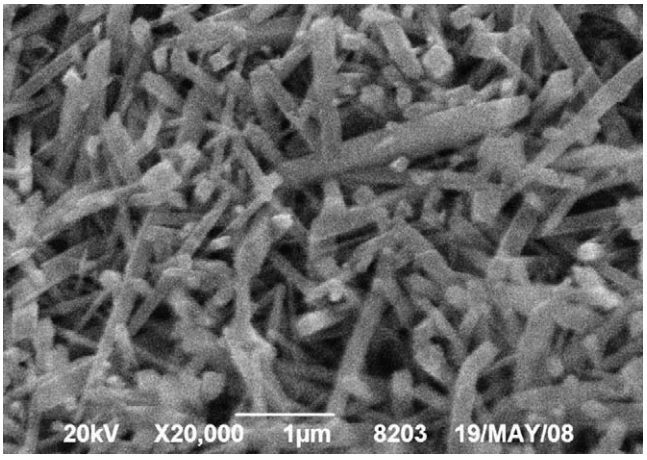

Fig. 6. SEM micrograph of crystallized sample at 1050 K.

The crystal morphology in the crystallized sample was investigated by SEM. A SEM micrographs of a sample crystallized at 1050 K are shown in Fig. 6 as an example. Rod-like crystals with about 0.1 μm × 0.1 μm × 2 μm in size occurred uniformly in the sample. Therefore, the result of SEM is consistent with the crystallization kinetics.

4. Conclusions

Thermal behavior and non-isothermal crystallization kinetics of 5MgO–9BaO–33B_2O_3–33Al_2O_3–20SiO_2 (mol%)

glass were investigated by dilatometry, DSC, XRD and SEM. The value of glass fragility index F indicates that the glass is formed from a kinetically stable liquid. Activation energy for glass transition was determined to be 206.1 kJ/mol. Crystallization activation energies for the glass was calculated to be 45.19 kJ/mol. The crystal growth was found to be controlled by a three-dimensional mechanism. $Al_4B_2O_9$ was precipitated first from the glass matrix at about 1000 K. At higher temperature, the metastable $Al_4B_2O_9$ phase partially transforms to stable $Al_{20}B_4O_{36}$.

Acknowledgments

The work was supported under the Hunan Natural Science Foundation: No. 08JJ4013. We thank Mr. Hong XiuCheng and Ms. Wu Yin for the DSC and XRD measurements of the glasses.

References

[1] H. Yusuke, N. Tomohiro, F. Kohei, K. Naoyuki, N. Junji, S. Akihiko, H. Kazuyuki, Thermo-optic properties of B_2O_3 doped Li_2O–Al_2O_3–SiO_2 glass–ceramics, J. Non-Cryst. Solids. 354 (27) (2008) 3113–3119.

[2] Esmat M.A. Hamzawy, A.F. Ali, Sol–gel synthesis and crystallization of aluminum borosilicate, Ceram. Int. 27 (6) (2001) 607–613.

[3] L. Zhe, W. Ruifang, H. Xiqang, L. Chaoqian, W. Bo, S. Wenhui, Oxygen pump method for leak rate testing of SiO_2–B_2O_3–Al_2O_3–BaO–PbO_2–ZnO glass sealant for SOFC, Solid State Ion. 179 (27/32) (2008) 1286–1290.

[4] X. Liu, Y. Wang, Some characteristics of glass in the Al_2O_3–B_2O_3–SiO_2 system from the gel, J. Non-Cryst. Solids 80 (1/3) (1986) 564–570.

[5] D.R. Peacor, R.C. Rouse, E.S. Grew, Crystal structure of boralsilite and its relation to a family of boroaluminosilicates, sillimanite, and andalusite, Am. Mineral. 84 (7/8) (1999) 1152–1161.

[6] R. Zheng, S.R. Wang, H.W. Nie, T.-L. Wen, SiO_2–CaO–B_2O_3–Al_2O_3 ceramic glaze as sealant for planar ITSOFC, J. Power Source 128 (2) (2004) 165–172.

[7] G. Ruitenberg, Applying Kissinger analysis to the glass transition peak in amorphous metals, Thermochim. Acta 404 (1/2) (2003) 207–211.

[8] M.M. Wakkad, E.Kh. Shokr, S.H. Mohamed, Optical and calorimetric studies of Ge–Sb–Se glasses, J. Non-Cryst. Solids 265 (2) (2000) 157–166.

[9] R. Bohmer, C.A. Angell, in: R. Richert, A. Blumen (Eds.), Disorder, Effects on Relaxation Processes, Springer, Berlin, 1994.

[10] R. Iordanova, E. Lefterova, I. Uzunov, D. Klissurshi, Non-isothermal crystallization kinetics of V_2O_5–MoO_3–Bi_2O_3 glasses, J. Therm. Anal. Cal. 70 (2002) 393–404.

[11] C.S. Ray, W.H. Huang, D.E. Day, Crystallization kinetics of a lithia-silica glass: effect of sample characteristics and thermal analysis measurement techniques, J. Am. Ceram. Soc. 74 (1) (1991) 60–66.

[12] T. Ozawa, Bull. Chem. Soc. Jpn. 38 (1965) 1881–1886.

[13] H.S. Chen, A method for evaluating viscosities of metallic glasses from the rates of thermal transformations, J. Non-Cryst. Solids 27 (2) (1978) 257–263.

[14] D. Mazza, M. Vallino, G. Busca, Mullite-type structures in the systems Al_2O_3–Me_2O (Me = Na, K) and Al_2O_3–B_2O_3, J. Am. Ceram. Soc. 75 (1992) 1929–1934.

[15] G. Werding, W. Schreyer, Synthesis and stability of werdingite, a new phase in the system MgO–Al_2O_3–B_2O_3–SiO_2 (MABS), and another new phase in the ABS-system, Eur. J. Mineral. 4 (1992) 193–207.